Self-Association in the Myosin System at High Ionic Strength. II. Evidence for the Presence of a Monomer ⇌ Dimer Equilibrium*

Jamie E. Godfrey† and William F. Harrington

ABSTRACT: High-speed sedimentation equilibrium studies of myosin in high salt concentration (0.5 M KCl–0.2 M PO_4^{2-}) are reported, providing evidence for the presence of a rapidly reversible, monomer–dimer equilibrium in this solvent. A computer program of Roark and Yphantis has been employed to derive $1/M_n$, $1/M_w$, and $1/M_z$ *vs.* concentration plots from experiments at various cell-loading concentrations (0.3–2.2 mg/ml) and rotor speeds (9,000–12,000 rpm). These plots all show distinct minima in the low concentration range ($< \sim 0.5$ mg/ml) with apparent convergence of the three reciprocal moments at zero concentration. Analysis of the averaged apparent reciprocal moments from 21 meniscus-depletion experiments indicates a concentration dependence consistent with a highly nonideal monomer–dimer equilibrium with a monomeric molecular weight for myosin of 458,000, an equilibrium constant, $K_2 = 9.98$ dl/g (at 6°) and a virial coefficient, $B = 6.60 \times 10^{-6}$ mole dl/g^2.

A very slow reaction leading to the formation of a higher molecular weight, pressure-sensitive n-mer (tetramer $< n$-mer $<$ decamer) has been detected in these systems. The possible significance of the myosin dimer as well as the higher n-mer in filament formation is considered.

Evidence for the presence of pH and phosphate ion-dependent self-association reactions of myosin at high ionic strength has been provided in the previous paper (Godfrey and Harrington, 1970). In the study to be reported below, we present data from high speed sedimentation equilibrium experiments demonstrating the presence of a myosin dimer which is in rapid, reversible equilibrium with monomeric myosin under these high salt concentration conditions. We believe the dimer to be the first intermediate in myosin thick filament formation. Moreover, it appears that its existence in significant concentration at high ionic strength has undoubtedly been a source of confusion in past efforts at determining the molecular weight of myosin.

Materials and Methods

Purification of Myosin. For the high-speed sedimentation equilibrium experiments, myosin from rabbit back muscle prepared as described earlier (see Godfrey and Harrington, 1970) was further purified by passage through DEAE-Sephadex A-50 (Pharmacia) according to the procedure of Richards *et al.* (1967). A 30 × 2.5 cm^2 column was equilibrated at 4° with 0.15 M phosphate–0.01 M EDTA, pH 7.5; 250–350 mg of myosin dialyzed against the same buffer was applied and eluted by a linear KCl gradient (450 ml of buffer and 450 ml of buffer made 0.5 M in KCl). The elution profiles at 280 mμ were very similar to those reported by these authors with three smaller peaks consistantly appearing in addition to the large myosin-containing peak (Figure 1). Any 5′-adenylic deaminase activity present in the myosin applied to the column was eluted in the void volume; no activity was ever found in the main myosin peak. Fractions from the trailing side of this peak (shaded portion in Figure 1) were selected for the sedimentation equilibrium experiments; prior to use these samples were exhaustively dialyzed against 0.5 M KCl–0.2 M phosphate–0.01 M EDTA (pH 7.3), diluted as required, and centrifuged at 25,000 rpm for 1 hr or more. The myosin at the beginning of each experiment was never more than 7-days old from the date of sacrifice.

Synthetic boundary cell experiments (see Materials and Methods in Godfrey and Harrington, 1970) were performed on solutions of chromatographed myosin in 0.5 M KCl–0.2 M PO_4^{2-}–0.01 M EDTA (pH 7.3) and their $OD_{280-320}$ values were accurately measured. Assuming dn/dc_{540} to be the same for chromatographed and unchromatographed myosin, $\epsilon_{280}^{1\%}$ was calculated for chromatographed myosin by the relation:

$$\epsilon_{280}^{1\%}{}_{\text{chr}} = \epsilon_{280}^{1\%}{}_{\text{unchr}} (\Delta J_{\text{unchr}}/\Delta J_{\text{chr}})(\text{OD}_{\text{chr}}/\text{OD}_{\text{unchr}})$$

The extinction coefficient for chromatographed myosin in the above solvent system was found to be 5.20 optical density units $\%^{-1}$ cm^{-1}, about 6% lower than $\epsilon_{280}^{1\%}$ for unchromatographed myosin (see Table I in Godfrey and Harrington, 1970).

Sedimentation Equilibrium Techniques. EVIDENCE FOR A REVERSIBLE MONOMER ⇌ DIMER EQUILIBRIUM. A substantial number of self-associating protein systems have been characterized recently through extensive analysis of sedimentation equilibrium data. A principle problem in many cases has been to correctly identify the mode of aggregation (*e.g.*, monomer–dimer, monomer–trimer–hexamer), a task that becomes dramatically more difficult when more than two species are present. However, in analyzing reversible monomer–dimer (M–D) systems which exhibit pronounced nonideality in solution, the principle problem can be detection of the self-association itself,

* Contribution No. 581 from the Department of Biology, McCollum Pratt Institute, The Johns Hopkins University, Baltimore, Maryland. *Received August 27, 1969.* This investigation was supported by U. S. Public Health Service Grant No. AM-04349. One of us (J. G.) gratefully acknowledges a U.S. Public Health Service predoctoral fellowship.

† Present address: Polymer Department, Weizmann Institute of Science, Rehovoth, Israel.

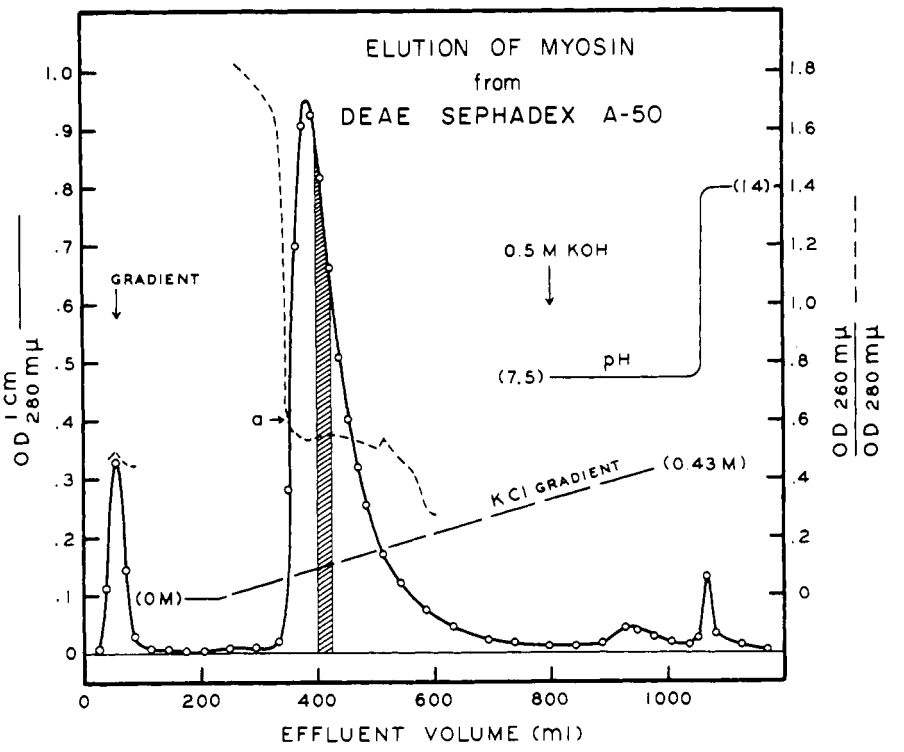

FIGURE 1: Typical elution profile of myosin from DEAE-Sephadex A-50. The conditions employed were: myosin (18 ml, 1.4%, 250 mg) on a 30 cm × 2.5 cm² column; elution by KCl linear gradient: 450 ml of 0.15 M PO_4^{2-}–0.01 M EDTA, pH 7.5 (equilibrating buffer), plus 450 ml of the same made 0.5 M in KCl; 4°; 15-ml fractions; a: 260 mμ/280 mμ from unchromatographed myosin. The shaded area represents the fractions used in high-speed sedimentation equilibrium experiments.

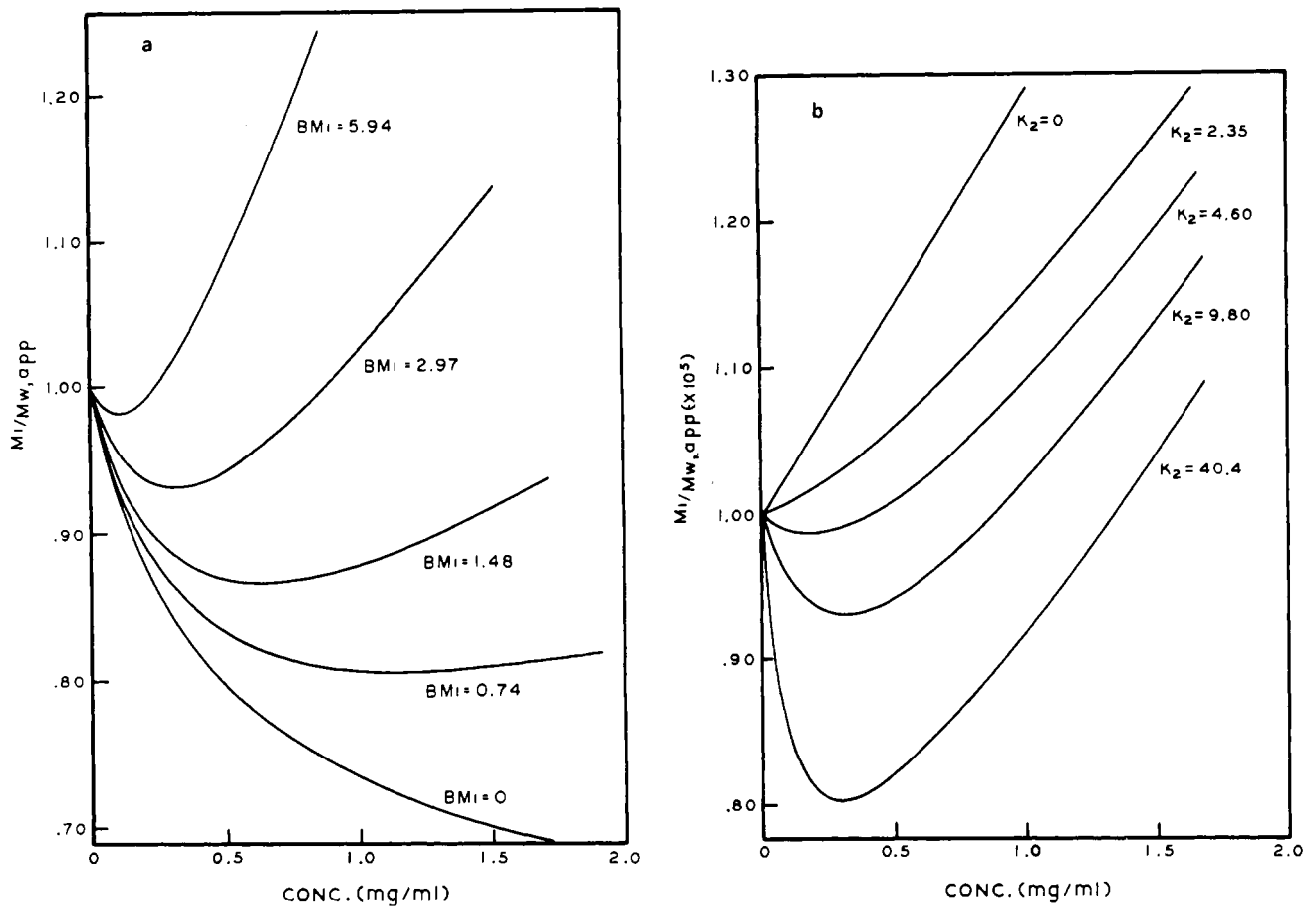

FIGURE 2: Simulated $M_1/M_{w,app}$ *vs.* concentration for M–D reversible association: (a) BM_1 varied, k_2 = 9.80 dl/g; (b) k_2 varied, BM_1 = 2.97 dl/g.

particularly when formation of the dimer is strongly favored. The theoretical M–D plots of Figure 2 clarify the difficulties involved. In Figure 2a, the virial coefficient is varied for a system with an association constant of 9.8 dl/g; and in Figure 2b, K_2 is varied for a system of constant nonideality (BM_1 = 2.97 dl/g). When $k_2/BM_1 > 1$, such plots of nonideal M–D systems will contain a minimum at some concentration value. At that concentration, the association reaction leading to higher weight-average molecular weights with increasing concentration is exactly counterbalanced by the nonideality of the system tending to reduce the apparent weight. At lower concentrations, the association reaction predominates, but at higher concentrations the virial coefficient prevails. It can be been that at moderately high values of BM_1 and K_2, the minimum in $M_1/M_{w,app}$ will be located below the effective concentration ranges of the low- and intermediate-speed sedimentation equilibrium methods. Moreover, $1/M_{w,app}$ at concentrations above the minimum will appear nearly linear further disguising the true nature of the system. Thus the reversible association may remain undetected and, in addition, the extrapolated infinite dilution "molecular weight" differ substantially from the true value of M_1. The error involved will depend upon the values for B and K_2, and the concentration range of the experimental data used in the extrapolation. To analyze these systems successfully, therefore, the high-speed meniscus-depletion technique must be employed and accurate data obtained in the very low (<0.1%) concentration region.

The presence of minima in plots of the reciprocal averages ($1/M_{n,app}$, $1/M_{w,app}$, $1/M_{z,app}$) and their convergence at a common infinite dilution value do not alone unequivocally demonstrate reversible association. The $1/M_{app}$ *vs.* c distributions described by a self-associating system can be duplicated by a disperse system of proper composition run at a particular cell-loading concentration and equilibrium rotor speed (ω). But under other conditions of rotor speed and c_0 such a system will describe quite different $1/M_{app}$ distributions. In contrast, the $1/M_{app}$ functions for all rapidly reversible associations including highly nonideal behaving ones, are independent of variations in these experimental parameters; the molecular weight moments are unique functions of concentrations (c_r) alone. For these systems, a series of meniscus-depletion experiments run under different conditions of rotor speed and c_0 will give identical $1/M_{app}$ *vs.* c plots as far as they extend. This test for rapid reversibility is most sensitive when experiments at the highest permissible values for c_0 and ω are compared with those at the lowest permissible values for these parameters. Between these two extremes in run conditions the reciprocal apparent functions for disperse systems can be expected to undergo maximum change.

High-speed meniscus depletion (or near depletion) experiments were carried out according to the procedure of Yphantis (1963). A Beckman Model E ultracentrifuge equipped with the electronic speed-control unit was aligned following the procedure outlined in the instrument manual; the standard width, symmetrical interference mask was used in all experiments. Aluminum-filled epon double-sector cells (12 mm) were filled with solution and dialysate to a column height of 2.7 mm (100 μl) using a 0.1-ml Hamilton precision syringe; FC-43 was not used because of its potential protein denaturing effect (Adams, 1967b). Moderate initial overspeeding for up to 14 hr at 1.2 times the equilibrium speed was employed in most cases. Equilibrium was achieved in 2.5–3.5 days as evidenced by fringe stability over an interval of 9 hr or more. Rayleigh patterns were recorded on Kodak Metallographic plates exposed for 15–30 min. Blank runs were made without disassembling the cells by repeatedly flushing out and finally filling the solution sector with dialysate to the level of the adjacent dialysate column. If discrepancies were noted in the meniscus levels after bringing the rotor to speed, the run was stopped and appropriate adjustments made in the levels of the "solution" sectors. Photographs of blank runs were taken after a lapse of 12 hr or more at speed. This procedure effectively removed all traces of protein from the solution sector as demonstrated by comparison of blank runs made before and after the equilibrium runs; their fringe patterns were invariably identical to within a few microns.

Rayleigh patterns were measured on the Nikon microcomparator with plates aligned on the reference hole air fringes. Concentrations were measured by averaging readings from three adjacent fringes at radial intervals varying from 200 to 25 μ, depending upon the concentration gradient. From 40 to 65 such triplets were read from each experimental run, 20 to 25 from the corresponding solvent blank. This unusually large number of data pairs was then analyzed by the Fortran IV high-speed equilibrium ultracentrifugation computer program of Roark and Yphantis (1969), a copy of which was kindly provided by Dr. Yphantis.

This program constitutes a significant advance over the more conventional methods of analysis and proved to be essential for the success of this study. It smooths the raw data by a sophisticated subroutine involving a sliding least-squares fit of 10 or more data pairs to a polynomial, either linear, quadratic, or cubic. Both the number of points taken and the degree of the polynomial fitted is dependent on the concentration gradient and the concentration span covered. This process is repeated with a cubic fit after each point has been assigned a weighting factor based upon its deviation from the previous fit. Each radial point is then assigned a new concentration value (rarely deviating by more than 5 μ of fringe displacement from the raw data value) derived from the polynomial fit for which it was the center (or near center) datum; the slope at the point is also calculated from the first derivative of the same cubic expression. From these concentration and gradient values, the various moments ($\sigma_{n,app}$, $\sigma_{w,app}$, etc., where $\sigma = \omega^2 M(1 - \bar{v}\rho)/RT$) are calculated at each radial point beginning at approximately 0.09 mg/ml of total protein concentration.

In nearly all experiments, meniscus depletion was effectively achieved as evidenced by a zero concentration gradient in the region below the meniscus; this conclusion was consistently concurred in by the computer program's subroutine which estimates the meniscus concentration from an analysis of the gradient in this region. The largest meniscus concentration so estimated was 5 μg/ml (6 μ of fringe displacement) for runs under conditions of high cell-loading concentration and low rotor speed. The maximum measurable concentration at the bottom of the column varied, depending on run conditions, from 1.5 (about 6 fringes) to 3.0 mg per ml. The pronounced nonideal behavior of the myosin system was responsible for these relatively large concentration spans.

The results obtained from the meniscus-depletion experiments within the low concentration region stand at the edge of credibility by current standards of centrifugation technique. The precision reported for the molecular weight values in this range, therefore, merits further comment; in addition, some

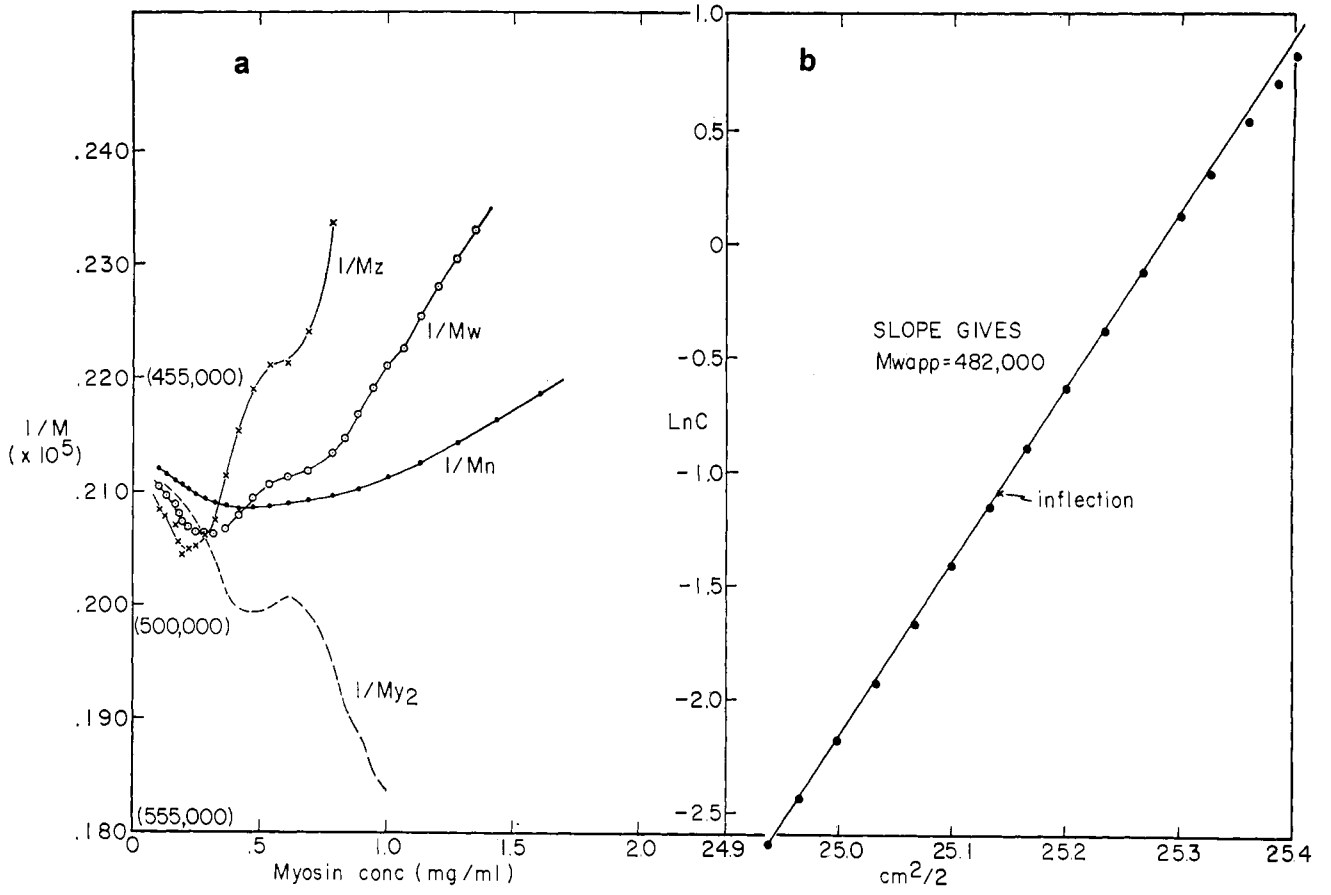

FIGURE 3: (a) Roark and Yphantis computer program analysis of high-speed sedimentation equilibrium run of myosin solution with minimal concentration of higher *n*-mer. The loading concentration was: 2.2 mg/ml of myosin in 0.5 M KCl–0.2 M PO_4^{2-}–0.01 M EDTA, pH 7.3; 12,000 rpm; 6°. Many data points were omitted. (b) ln *c vs.* r^2 of the data in a. Concentration is given in millimeters of fringe displacement.

potential sources of artifact, safely ignored in most systems, should be evaluated.

It is widely accepted that the usual ln *c vs.* r^2 analysis of most systems give values reproducible to about ±4%. But at the low concentrations where the monomer-dimer upturn occurs (see Figure 3a) the scatter is significantly greater due principally to the dependence of $M_{w,app}$ on $1/c$. Thus, a 5-μ error at 500 μ of fringe displacement (*ca.* 2 fringes) produces a 1% error in $M_{w,app}$, but the same 5-μ deviation at 100 μ of fringe displacement leads to a 5% error in $M_{w,app}$. The averaging of the results from 21 runs is largely responsible for increasing the confidence in the data at these low concentrations; however, two other factors contributed to the precision of the individual runs: (1) the procedure adopted for the dialysate blank runs, and (2) the reproducibility of the comparator readings. The former eliminated the optical errors introduced when cell windows are reseated between solution and dialysate runs. Filling each limb with solvent (in this case, quite high in salt) ensured that inequalities in the two sector path lengths would be fully reflected in the blank Rayleigh patterns. The precision in measuring fringe displacements on the microcomparator was such that the middle fringe reading at each radial position rarely deviated by more than 3 μ from the average of the three fringe values.

Wiener skewing is undoubtedly a finite source of error in these results. The midplane focal point, the compromise suggested by the Spinco manual to accommodate the requirements of both the schlieren and Rayleigh optical systems, does lead to spurious fringe deviations which are all but eliminated when the focal plane is at the two-thirds level. The general effect of Wiener skewing is to impose a very mild dimerization effect on the data which is roughly proportional to the cell path length and σ^2 [(d ln c/d(r^2/2))^2, Yphantis (1964)]. Since the two sets of averaged results at the high- and low-speed conditions with the σ^2 differing by a factor of 2.3 at the two rotor speeds are essentially the same, it seems unlikely that Wiener skewing is causing a significant error. Moreover, the intermediate-speed experiments with the KCl–PO_4 solvent system described in the previous paper (Godfrey and Harrington, 1970) gave cell-average apparent molecular weights consistent with the values from the high-speed runs although the σ values for these two series of runs differed by a factor of 7.1.

Convection within the solution column can be a problem in sedimentation equilibrium experiments at speeds too low to create an adequate salt density gradient. Borderline conditions have been reported (Yphantis, 1964) to be about 17,000 rpm with a 0.1 M salt solvent system; but, because the gradient

formed is directly proportional to concentration, a 0.5 M salt solvent system could be run at 7500 rpm—one fifth the centrifugal field generated at 17,000 rpm—and the same gradient would be present. The experiments described herein, therefore, meet the minimal requirements for an adequate salt gradient. Rotor wobble can also promote convection and the results from a few experiments were discarded when discernible wobble was detected either during the run itself or in the run immediately following. Although often complex, the usual effects of convection are to "wash out" the low concentration gradient region giving downturn, rather than upturn, in the $1/M_{app}$ functions with decreasing concentration (Yphantis, 1964). This phenomenon was observed in the $1/M_{w,app}$ plots from one or two of these rejected experiments.

Chemical equilibrium within the solution is necessary in order to achieve meaningful concentration distributions at sedimentation equilibrium. In the phosphate solvent system and in KCl alone, it is clear that slow reactions are taking place leading to higher n-mer species; it is also clear that the reaction rate in the presence of phosphate is significantly retarded over that in the standard KCl solvent. The Rayleigh patterns from the phosphate runs did not show detectable change over intervals of 9 hr or more after equilibrium had been reached even though after 72 hr, a definite increase in the higher n-mer concentration has occurred. In addition, common convection related effects which are likely to result from continuous aggregation within the solution column were never seen except in those runs in which rotor wobble was suspected (see above). Thus, the proforma criteria for sedimentation equilibrium seem to be fulfilled.

Results

Twenty-one, high-speed meniscus-depletion experiments with myosin in KCl–PO_4^{2-} solvent were carried out at different cell-loading concentrations (0.3–2.2 mg/ml) and rotor speeds (9,000–12,000 rpm); all runs were conducted at 6°. These runs include all members of the series not rejected for known defects (rotor wobble, optically unstable cell windows) except two at low rotor speed and low cell-loading concentration; the reasons for their exclusion will be discussed later (see Figure 9g and descriptive text).

Figure 3a presents results from one run (12,000 rpm and 2.2-mg/ml cell-loading concentration) analyzed by the Roark and Yphantis computer program, and Figure 3b shows the ln c *vs.* r^2 plot of the same data. The latter exhibits noticeable downward curvature only at the high concentration end; although it appears linear throughout the remainder of its length, the function is, in fact, sigmoidal in shape with the inflection point as indicated. This point, with the highest slope, corresponds to the minimum in the reciprocal apparent weight-average curve. It occurs at a concentration (about 0.3 mg/ml) below that found at the meniscus of any of the LaBar intermediate-speed experiments described in the previous paper. The downward curvature in the ln c *vs.* r^2 function above the inflection expressing the nonideality of the system is reflected in the increasing values of the three reciprocal averages at higher concentrations. Below the inflection point, $1/M_{w,app}$ again increases as it approaches zero concentration where all three reciprocal moments appear to converge. These minima in the three reciprocal averages within the low concentration region were seen in the plots from all 21 experiments.

The descending curve of Figure 3a is the reciprocal of the M_{y2} average which is defined as:

$$M_{y2} = (M_{w,app})^2/M_{z,app} \quad (1)$$

This expression defines a molecular weight moment with the second virial coefficient eliminated mathematically, although higher virial terms are not (see Roark and Yphantis, 1969). For a nonideal, associating system $1/M_{y2}$ will continue to decrease beyond the concentration of the minimum, as it does here. This behavior in the $1/M_{y2}$ function was seen in all of the high-speed sedimentation equilibrium experiments.

The perturbation at about 0.6 mg/ml in the $1/M_{y2}$, $1/M_{z,app}$, and $1/M_{w,app}$ curves indicates the presence of a particular higher n-mer in significant concentration. This evidence of a larger species appears to a greater or lesser degree in the molecular weight distributions of every run and will be considered in detail below.

When the results from the 21 runs are averaged at ten concentrations within the 0.09–0.50 mg/ml range, they give the three sets of points (unbracketed) for $1/M_{n,app}$, $1/M_{w,app}$, and $1/M_{z,app}$ presented in Figure 4. Of the over 3000 pairs of individual comparator readings which were analyzed 2000 fell within the concentration range shown here. The error bars, spanning approximately $\pm 1\%$ of the molecular weight values, indicate 95% confidence limits for the apparent weight-average molecular weights at the different concentrations. They do not reflect the confidence estimates set by the computer program for the values from each run, but are based rather upon the standard deviations from the mean of all 21 $1/M_{w,app}$ values at each concentration.

The strong indication of convergence of the three reciprocal moments to a reasonably high molecular weight value at infinite dilution indicated reversible association, rather than contamination of the system by low molecular weight material. Moreover, the very low concentration region in which the three minima occur further suggested that monomer–dimer was the most likely mode of aggregation since the minima in the reciprocal moments of higher modes of aggregation will occur at higher concentration values unless the association constants and virial coefficients are extremely large. This hypothesis was also consistent with the sedimentation velocity results presented in paper I of this series (Godfrey and Harrington, 1970). Accordingly, the $1/M_{app}$ functions were analyzed initially assuming that a monomer–dimer self-association was present. To determine the three parameters which define such a system, *i.e.*, the molecular weight of the monomer (M_1), the association constant (k_2), and the virial coefficient (B), the following three relationships were used.

$$1/M_{w,app} = 1/2M_1 + 1/[2M_1(4k_2c + 1)^{1/2}] + Bc \quad (2)$$

$$1/M_{n,app} = 1/2M_1 + 1/\{M_1[(4k_2c + 1)^{1/2} + 1]\} + (1/2)Bc \quad (3)$$

$$M_1 = k_2/(B(4k_2c + 1)^{1/2}) \quad (4)$$

Equations 2 and 3 are modifications of the two-term virial expressions for the number and weight apparent moments in which $1/M_{n,c}$ and $1/M_{w,c}$ have been expressed in terms of M_1, k_2, and the concentration, c. The derivations of eq 2

TABLE I: Monomer–Dimer Reversible Association Parameters for Myosin in 0.5 M KCl–0.2 M PO_4^{2-}–0.01 M EDTA, pH 7.3 at 6°. Analysis of Data from 21 High-Speed Sedimentation Equilibrium Experiments.

Parameter	Calcd Value
M_1	458,000 g/mole
B	6.60×10^{-6} mole dl/g^2
BM_1	3.02 dl/g
k_2	9.98 dl/g
	2.29×10^5 l/mole

and 3 assume equivalence of the virial coefficients of monomer and dimer, $B_1 = B_2$.[1] Equation 4 is the first derivative of $1/M_{w,app}$ with respect to c (eq 2) set equal to zero. It is useful for systems where $1/M_{w,app}$ goes through a minimum value at some finite concentration and applies only at that concentration. The two-term virial expression for the apparent z-average moment (eq 5) could have been used in determining the parameters, but, for reasons given below, it was considered to be less reliable for this purpose.

$$1/M_{z,app} = \left[\frac{1}{2M_1 - \left(\frac{M_1}{(4k_2c + 1)^{1/2}}\right)}\right] \times \left[1 + \frac{1}{\left(\frac{1}{2BM_1c}\right) + \left(\frac{1}{2BM_1c(4k_2c + 1)^{1/2}}\right)}\right] \quad (5)$$

Two approaches are possible with these equations: (1) When M_1 is estimated independently by smooth extrapolation of $1/M_{n,app}$ to zero concentration—the average which approaches infinite dilution least acutely—a value of 458,000 is obtained. With this quantity then inserted, any two of the equations (preferrably 2 and 3) can be solved simultaneously to yield B and k_2. (2) Alternatively, all three equations can be solved simultaneously to give M_1 as well as k_2 and B. For this calculation, data at the concentration of the $1/M_{w,app}$ minimum was used [(points a and b) Figure 4]. The latter approach has the advantage of utilizing experimental data only from the upturn region which, as suggested by the confidence limits, are probably more reliable; the extrapolation at an acute angle to zero concentration employing values at lower concentrations is thus obviated. It should be added that M–D systems with much lower k_2 values are best analyzed by the former method since the required extrapolation to determine M_1, in these instances, can be quite accurate. Both methods yield the same values for the three parameters (Table I).

The capacity of the data at a single concentration some distance from the ordinate to so accurately predict the extrapolation value of M_1 no longer seems surprising when

[1] See the papers of Adams and coworkers (Adams, 1965, 1967a,b; Adams and Filmer, 1966; Adams and Williams, 1964) for a discussion of the general procedure adopted for deriving these equations.

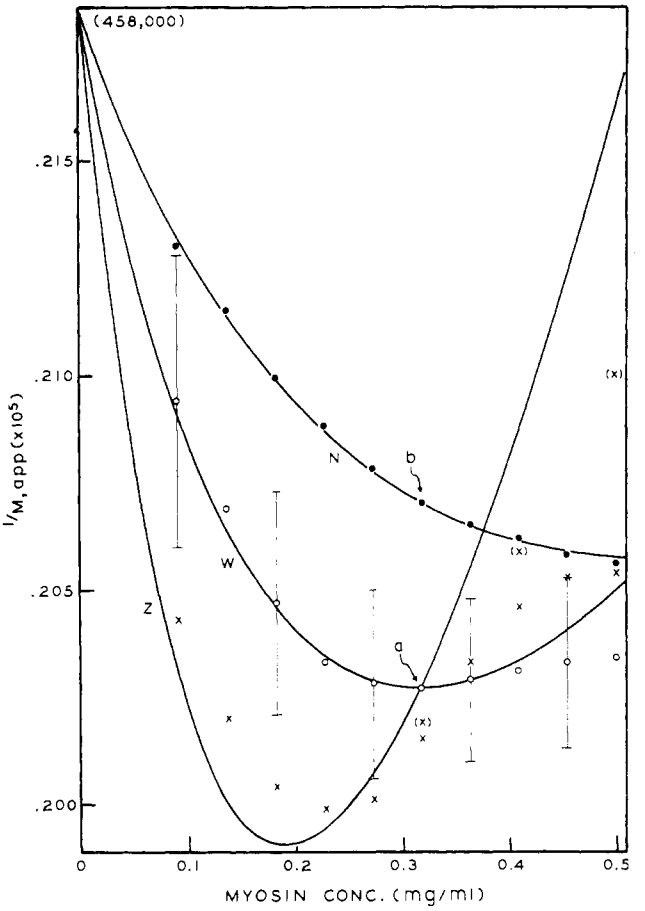

FIGURE 4: Averaged reciprocal moments *vs.* concentration from 21 high-speed sedimentation equilibrium runs with simulated moments obeying parameter values in Table I. Points are experimental: ●, $1/M_{n,app}$; ○, $1/M_{w,app}$; ×, $1/M_{z,app}$; (×), from six runs at high-speed, high-loading conditions. Vertical bars are 95% confidence limits for $1/M_{w,app}$ mean values. Solvent was 0.5 M KCl–0.2 M PO_4^{2-}–0.01 M EDTA, pH 7.3; 6°, 9,000–12,000 rpm; curves: reversible M–D association, M_1 = 458,000, B = 6.60×10^{-6} mole dl/g^2, k_2 = 9.98 dl/g; points a and b, see text; $Z = 1/M_{z,app}$; $W = 1/M_{w,app}$; $N = 1/M_{n,app}$.

the computer-calculated reciprocal apparent molecular weight moments, defined by the three derived parameters, are superimposed on the averaged experimental values (solid curves in Figure 4). The agreement of the simulated and experimental apparent number and weight-average values is remarkable; the theoretical profile fits the $1/M_{z,app}$ points less precisely but is still within ±1% of the data. The bracketed $1/M_{z,app}$ points which more closely approach the simulated values are from runs under conditions of high rotor speed and high cell-loading concentration, conditions which more effectively separate the heavy and light species in the solution column at sedimentation equilibrium. Although present in all of the experiments, the higher n-mer contributes less to the total mass in the low concentration range of these particular runs. The influence of the higher weight species on the data points for the other two reciprocal moments can also be seen, but the effect (consistent with theory) is less dramatic.

Tests for other Association Modes. Other modes of aggre-

TABLE II: Analysis for Mode of Reversible Association[a] of Myosin in 0.5 M KCl–0.2 M PO_4^{2-}–0.01 M EDTA, pH 7.3, at 6°. Data from 21 High-Speed Sedimentation Equilibrium Runs.

Mode	Eq[b]	Concn (mg/ml)	B[c]	Calcd Value	Data Value	Difference (absolute)	% Difference
M–D	a	0.22	6.6	0.2015	0.2034	0.0019	0.93
	b	0.22	6.6	0.2031	0.2034	0.0003	0.15
	a	0.35	6.6	0.3181	0.3180	0.0001	0.03
	b	0.35	6.6	0.3152	0.3180	0.0028	0.88
							Av 0.46
M–D–T	c	0.22	6.6	0.1595	0.1638	0.0043	2.63
	d	0.22	6.6	2.134	2.158	0.024	1.11
	c	0.35	6.6	0.2400	0.2396	0.0004	0.17
	d	0.35	6.6	3.340	3.341	0.001	0.04
							Av 0.74
M–D–T–T	e	0.22	6.6	−0.699	−0.684	0.015	2.19
	e	0.35	6.6	−1.180	−1.185	0.005	0.42
							Av 1.31
M–T (trimer)	f	0.22	6.6	0.4687	0.4167	0.0520	12.4
	f	0.35	6.6	0.8251	0.6556	0.1695	25.9
							Av 19.2
	f	0.22[d]	15.8	0.4678	0.4167	0.0511	12.3
	f	0.35	15.8	0.6555	0.6566	0.0011	0.02
M–D–T	c	0.22	15.8	0.1606	0.1638	0.0032	1.95
	d	0.22	15.8	2.140	2.158	0.018	0.83
	c	0.35	15.8	0.2260	0.2396	0.0136	5.68
	d	0.35	15.8	3.190	3.341	0.151	4.52
							Av 3.25
M–D–T–T	e	0.22	15.8	−0.798	−0.684	0.114	16.7
	e	0.35	15.8	−1.632	−1.185	0.447	37.7
							Av 26.2

[a] Method of Adams *et al.* (1964, 1965, 1966, 1967a,b). [b] The equations used are: (a) $2cM_1/M_{n,app} - c = \alpha e^{-BM_1c} + BM_1c^2$; (b) $2cM_1/M_{n,app} - c = \psi + 2/[(M_1/cM_{w,app}) - BM_1] + BM_1c^2$; (c) $6cM_1/M_{n,app} - 5c = 2\alpha e^{-BM_1c} + 3BM_1c^2 - 1/[(M_1/cM_{w,app}) - BM_1]$; (d) $30cM_1/M_{n,app} - 19c = 12\ \alpha e^{-BM_1c} + \psi + 15BM_1c^2$; (e) $24cM_1/M_{n,app} - 26c = 6\alpha e^{-BM_1c} + 12BM_1c^2 - \psi - 9/[(M_1/cM_{w,app}) - BM_1)]$; (f) $3cM_1/M_{n,app} - c = \psi + 3/[(M_1/cM_{w,app}) - BM_1] + 3BM_1c^2/2$; where, $\alpha = c\ exp\left[\int_0^c (M_1/M_{w,app} - 1)dc/c\right]$ and $\psi = (d(M_1/cM_{w,app})/dc)/[(M_1/cM_{w,app}) - BM_1]^3$. [c] Values are $\times 10^6$ mole dl/g^2. [d] B adjusted to achieve fit at this concentration.

gation besides monomer–dimer could conceivably fit the experimental data. To explore this possibility, the data were analyzed by the procedure described by Adams (1967b). The data at two concentrations, one on each side of the $1/M_{w,app}$ minimum, fit almost exactly the test equations for monomer–dimer association using the value for B determined above. In addition, they fit test equations for both monomer–dimer–trimer (M–D–T), and monomer–dimer–trimer–tetramer (M–D–T–T) modes, of which M–D is a special case, with k_3 and k_4 equal to zero. These test equations and the results from them are presented in Table II.

The fit to the monomer–trimer equation, on the other hand, was much less satisfactory using the value for B derived from the monomer–dimer analysis. By increasing B by over twofold, the data at the higher of the two concentrations could be made to fit the M–T equation, but the new value for B did not give a good fit of the data at the lower concentration. Moreover, if the association were M–T, the data using the higher value for B should fit the test equations for M–D–T and M–D–T–T associations as well, but the fit was poor in both cases (see Table II). Test equations for monomer–tetramer and higher modes of aggregation give even less satisfactory fits forcing B to unrealistically high values in order to achieve agreement at a particular concentration.

The excellent fit of the M–D equations to the data and the lack of a better fit by the M–D–T or M–D–T–T equations strongly suggest that if trimer or tetramer are present, they must exist in very low concentrations (see Adams, 1967b, for criteria of selecting M–D over higher modes of aggrega-

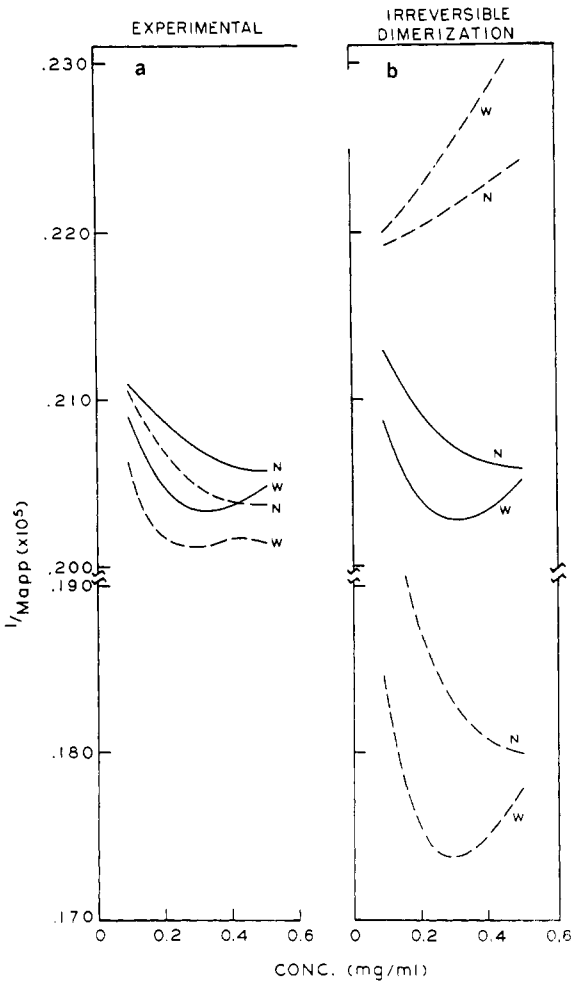

FIGURE 5: Experimental and simulated $1/M_{w,app}$ and $1/M_{n,app}$ *vs.* concentration at high-speed, high cell-loading and low-speed, low cell-loading conditions. (a) Averaged experimental values. Solid curves are from 6 runs at high-speed, high cell-loading; dashed curves are from 7 runs at low-speed, low cell-loading (see text for details). Solvent was 0.5 M KCl–0.2 M PO_4^{2-}–0.01 M EDTA, pH 7.3; 6°, 9,000–12,000 rpm. (b) Irreversible M–D system. Solid curves are for 41% dimer at low-speed, low cell-loading or 64% dimer at high-speed, high cell-loading conditions; dashed curves (below) are for 64% dimer at low-speed, low cell-loading; dashed curves (above) are for 41% dimer at high-speed, high cell-loading conditions. B and M_1 equal values in Table I. $W = 1/M_{w,app}$; $N = 1/M_{n,app}$.

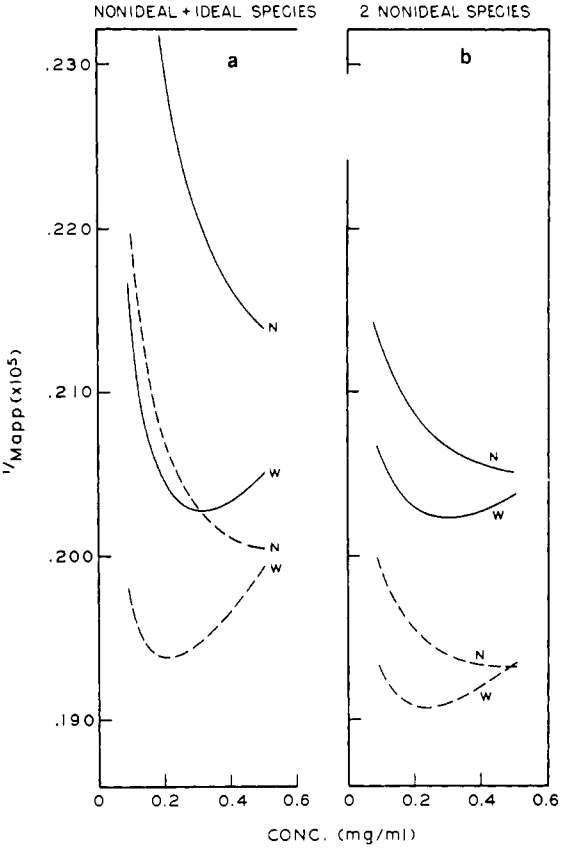

FIGURE 6: Simulated $1/M_{w,app}$ and $1/M_{n,app}$ *vs.* concentration at high-speed, high cell-loading and low-speed, low cell-loading conditions. (a) Nonideal species (M = 575,000; $B = 3 \times 10^{-6}$ mole dl/g²) plus 6% of an ideal species (M = 230,000); (b) nonideal species (M = 606,000) plus 23% of another nonideal species (M = 404,000); B for both species = 2.5×10^{-6} mole dl/g². Solid curves in a and b, at high-speed, high cell-loading conditions; dashed curves, at low-speed, low cell-loading conditions. $W = 1/M_{w,app}$; $N = 1/M_{n,app}$.

tion). Higher n-mers than tetramer cannot be ruled out on the basis of the data below 0.36 mg/ml (the highest of the two test concentrations) because significant concentrations of these species would not appear in this range unless their formation was highly favored (*i.e.*, k_n was very large). This conclusion is based upon considerations to be discussed below.

Two hypotheses other than a rapidly reversible monomer–dimer association could account for these data and must be disproved before the M–D thesis can be accepted: (1) a portion of the myosin is irreversibly aggregated to the dimer state, and, (2) small molecular weight contaminants are present at low concentration. In the latter case myosin would be required to have a significantly higher infinite dilution weight than 458,000. Figures 5 and 6 illustrate the basis for rejecting these alternative explanations.

As discussed earlier, it is a cardinal requirement for the demonstration of rapid reversibility in an associating system that the apparent molecular weight averages at any total protein concentration be constant, independent of either cell-loading concentration or rotor speed. The reciprocal apparent number- and weight-average molecular weights of 6 experiments from the 21 at high cell-loading concentration (averaging 2.06 mg/ml) and high rotor speed (12,000 rpm) were averaged at ten concentrations spanning the range 0.09–0.50 mg/ml giving the solid curves seen in Figure 5a. The dashed curves are the same data from seven experiments at low cell loading (averaging 0.47 mg/ml) and low rotor speed (averaging 9700 rpm). The upper curves of each pair are the $1/M_{n,app}$ distribution.

The two sets of $1/M_{app}$ values do not differ from each other by more than 1%. However, if the system contained irreversible dimer, the two sets of curves would be expected to appear as they do in Figure 5b. The calculated value for k_2 (9.98 dl/g) requires that 64% of the myosin in a reversible M–D system be in the dimer state at sedimentation equilib-

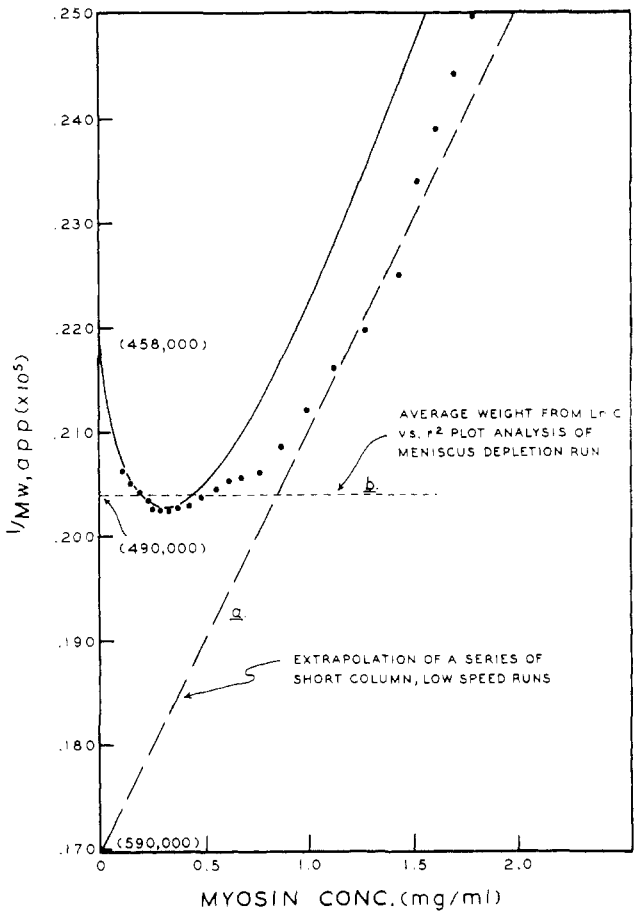

FIGURE 7: Effect of M–D reversible association on previous measurements of the molecular weight of myosin. ●: $1/M_{w,app}$ values from Roark and Yphantis computer program analysis of experiment with 2.2 mg/ml of myosin in 0.5 M KCl–0.2 M PO_4^{2-}–0.01 M EDTA, pH 7.3; 6°; 12,000 rpm; 350 μl of oil layered on solution and solvent columns to depress the amount of higher *n*-mer. Solid curve: $1/M_{w,app}$ for M–D reversible association obeying M_1, B, and K_2 values in Table I. (a) Extrapolation of $1/M_{w,app}$ values from a hypothetical series of low-speed, short-column sedimentation equilibrium experiments. (b) Cell-average $1/M_{w,app}$ (ln *c vs.* r^2 plot analysis) of a hypothetical high-speed sedimentation equilibrium experiment.

rium under the high-loading, high-speed conditions. Therefore, an *irreversible* system with the same proportion of dimer and run under these conditions would describe the solid curves seen in Figure 5b.[3] This system run at the low-loading, low-speed conditions, however, would give the lower dashed curves in Figure 5b. Conversely, at the low cell-loading, low-speed run conditions, a reversible M–D system with the above k_2 has only about 41% of its mass in the dimer form at sedimentation equilibrium. An *irreversible* system with this monomer–dimer ratio run at the high-loading, high-speed conditions would give the upper dashed curves in Figure 5b. Here, the order of the two averages is reversed because of the absence of minima.

[3] These distributions and those appearing in Figure 6 were generated by computer programs, written in our laboratory, designed to simulate apparent molecular weight moments for various model systems at sedimentation equilibrium.

The gross separation of the $1/M_{app}$ values to be expected at the two sets of run conditions from either analysis of the data makes an irreversible dimerization only a remote possibility. The difference of 1% between the experimental curves would indicate the presence of about 7% irreversible dimer or unreactive monomer in the myosin solutions; the isolation and purification procedure might easily be responsible for this level of denatured molecules.

In Figure 6a, the solid curves are the two reciprocal moments for a system in sedimentation equilibrium at the high cell-loading, high-speed conditions containing a non-ideal behaving species, M = 575,000 and $B = 3 \times 10^{-6}$ mole dl/g² (about one-half the virial coefficient calculated in the M–D analysis), plus an ideal behaving contaminant, M = 230,000, representing 6% of the total protein concentration. The molecular weights, virial coefficient, B, and the relative concentrations were adjusted so that the $1/M_{w,app}$ distribution would closely resemble the experimental results. The dashed curves are the reciprocal averages for the same system under the low-speed, low-loading run conditions. The principle feature that characterizes this and other systems of this general model is the divergence of the reciprocal averages seen most strikingly here in the $1/M_{n,app}$ curve at the high-speed, high cell-loading conditions. Lowering the molecular weight of the contaminant and its concentration (required to maintain a reasonable fit of the experimental $1/M_{w,app}$ function) tends to increase this divergency. On the other hand, increasing the molecular weight and concentration of the contaminant, although it lessens the divergency, makes detection of the smaller species a certainty by a variety of methods including sedimentation velocity.

Another model system would consist of two species closer in molecular weight and having the same second virial coefficient, possibly two types of myosin. Figure 6b presents curves for a system containing both a 606,000 and a 404,000 molecular weight species, the latter contributing 23% to the total concentration; for both, $B = 2.5 \times 10^{-6}$ mole dl/g². Again, the reciprocal apparent weight-average molecular weight at the high-loading, high rotor speed conditions approximates the experimental $1/M_{w,app}$ data; in this case, the reciprocal apparent number average also approaches its experimental counterpart. However, at the low-speed, low-loading conditions, the two curves are shifted significantly to lower values. Moreover, it is doubtful that the two species would sediment at the same rate at all cell-loading concentrations resulting in a single, sharp boundary in sedimentation velocity runs, even if the virial coefficient of the smaller species were higher. Narrowing the difference in weight between the two species makes fitting the experimental data at either set of run conditions increasingly difficult requiring a further depression of the assigned value for B.

The virial coefficients in the last two model systems, by necessity, are less than one-half of that determined in the reversible association analysis. Higher values would not allow a simulation of the experimental data by either model regardless of the values chosen for the species' molecular weights. Figure 7 shows the computer simulated reciprocal apparent weight-average molecular weight for the monomer–dimer association obeying the three derived M–D parameters carried to higher concentrations. Also included are the individual data points of a single representative run contaminated to only a minimal extent by the higher *n*-mer. It can

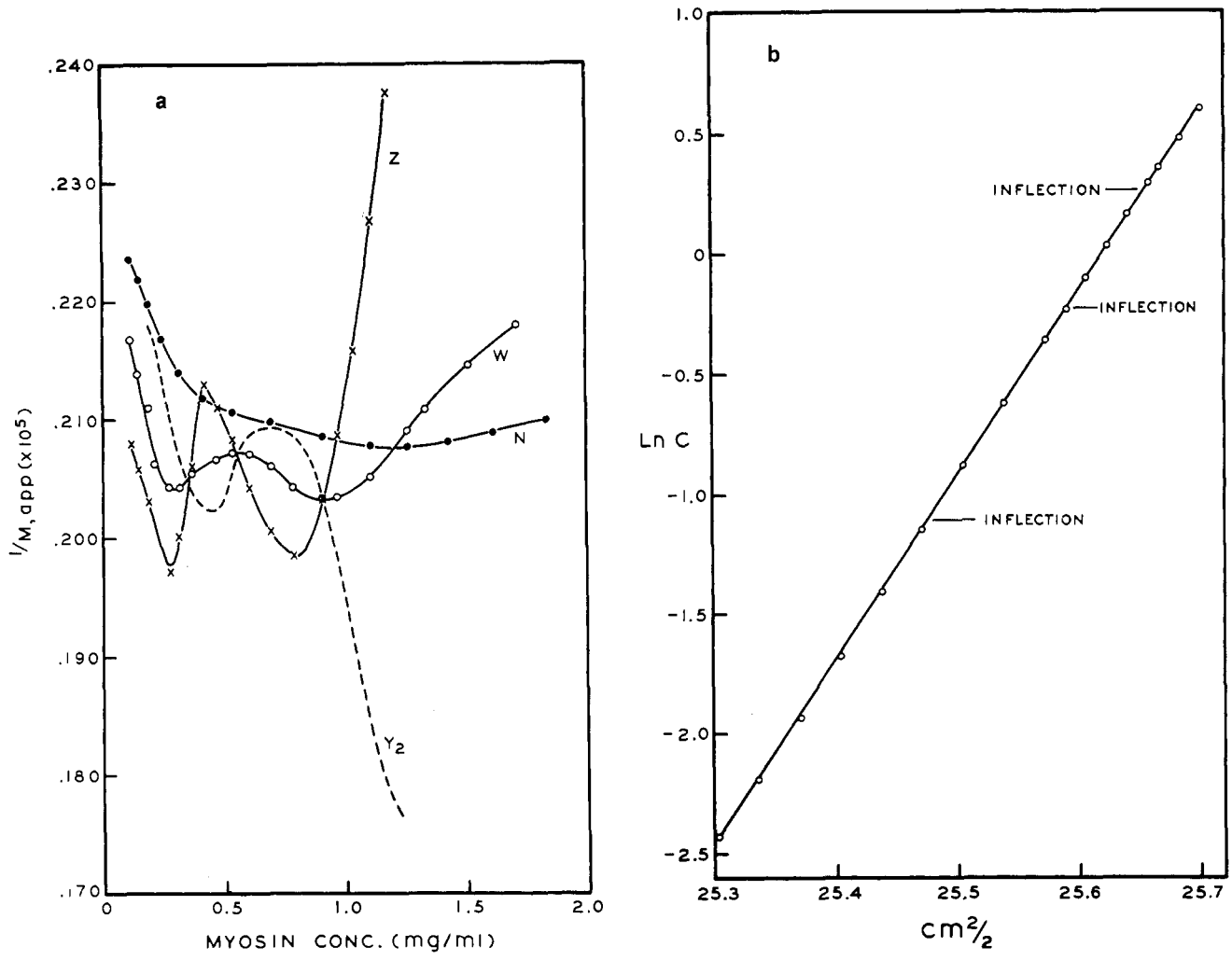

FIGURE 8: Roark and Yphantis computer program analysis of high-speed sedimentation equilibrium run of myosin solution with significant concentration of higher *n*-mer. (a) 0.52 mg/ml of myosin in 0.5 M KCl–0.2 M PO_4^{2-}– 0.01 M EDTA, pH 7.3; 12,000 rpm; 6°c. $Z = 1/M_{z,app}$; $W = 1/M_{w,app}$; $N = 1/M_{n,app}$; $Y_2 = 1/M_{y2}$. Many data points were omitted. (b) ln *c vs.* r^2 of the data in a.

be seen that a slope of less than one-half of that shown would be a much poorer fit of the experimental results. The presence of the heavier species acts to lower the slope of $1/M_{w,app}$ at concentrations above the minimum. Thus a B of less than 9.98 dl/g for the M–D system alone is unlikely.

These particular systems do not exhaust the possible alternative models for simulating the experimental results, but they are representative. Thus far, no others have been found which better duplicate the data.

To further investigate the possibility of the presence of low molecular weight material, myosin solutions of 1.5 mg/ml were brought to equilibrium at higher rotor speeds. At 34,000 rpm, giving about an eightfold increase in the field over that at 12,000 rpm, the amount of material distributed above the pelleted myosin was measured. Allowing for a smooth extrapolation of the concentration gradient through the pellet to the cell bottom, light material was found to contribute less than 0.5 of 1% to the total protein mass. At 18,000 rpm, in an experiment employing a 30-mm path-length cell and a solution column more than twice the length of that used in the lower speed runs (loading volume = 0.5 ml), no distribution above the pellet was detected. This evidence, added to the sedimentation velocity results cited previously (Godfrey and Harrington, 1970), seems to rule out the presence of significant amounts of light molecular weight contaminants.

Evidence for the Presence of a Higher n-mer Species. Turning now to an analysis of the molecular weight moments at concentrations above the M–D minimum, Figure 8a presents results from an experiment at lower loading concentration in which the amount of heavier species in the higher concentration range is substantially greater than that shown in Figure 3a. The $1/M_{y2}$ distribution is again included with the three common reciprocal averages.[4] A bizarre feature is seen: namely, the presence of a distinct, second minimum.

[4] Despite the mathematical elimination of B, $1/M_{y2}$ indicates a decrease in the molecular weight at certain concentrations when, clearly, the actual molecular weight in the solution column at sedimentation equilibrium is always increasing with concentration. This seeming anomaly arises from the definition of this moment (eq 1) which, with B eliminated, is essentially $M_{w,c}$ multiplied by the ratio $M_{w,c}/M_{z,c}$. This latter factor is not a simple linear function of total concentration for a nonideal associating system.

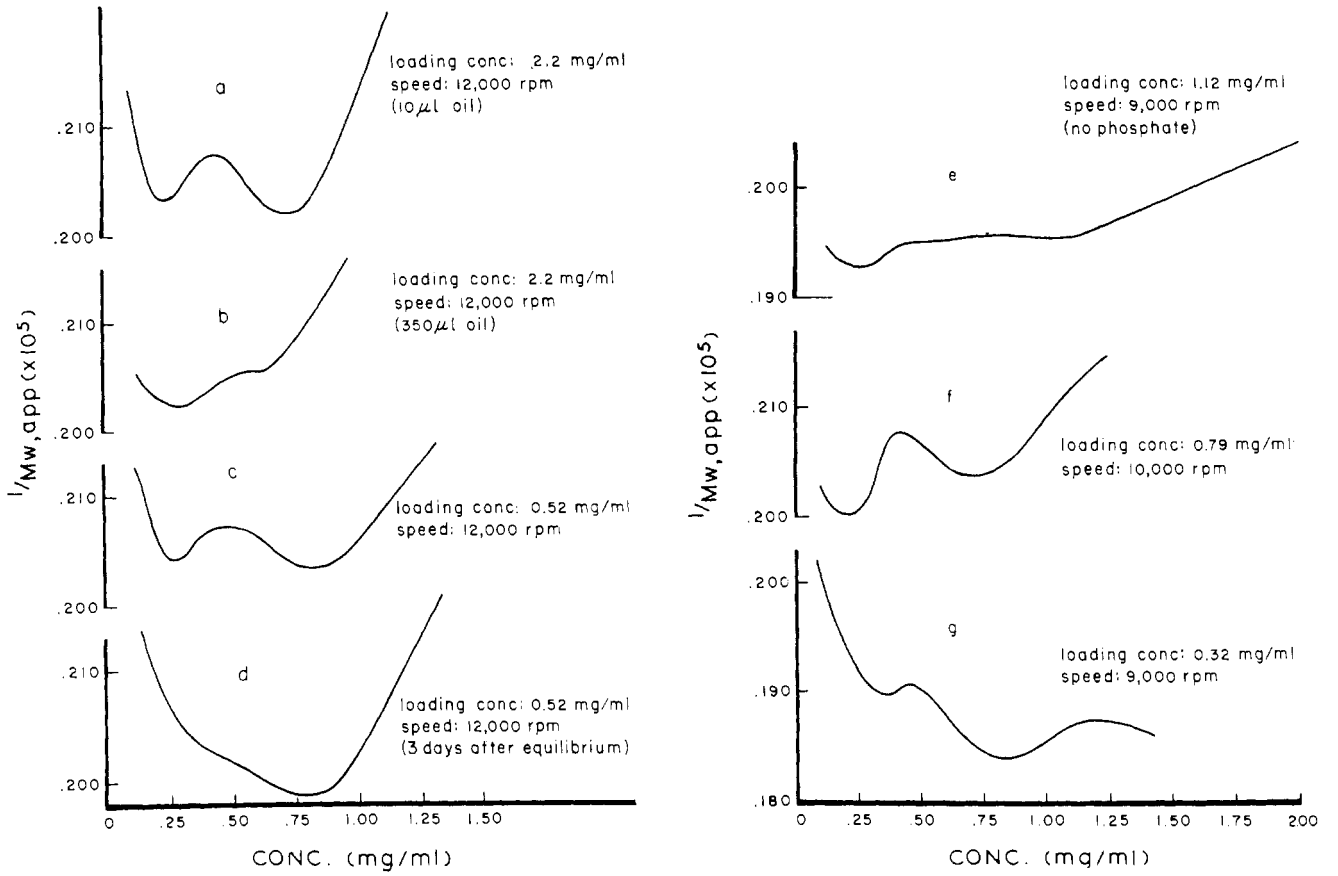

FIGURE 9: $1/M_{w,app}$ *vs.* concentration for myosin demonstrating the effect of various experimental and environmental parameters on the higher *n*-mer species. Solvent in all runs except e was 0.5 M KCl–0.2 M PO_4^{2-}–0.01 M EDTA, pH 7.3; solvent in e was 0.5 M KCl–0.01 M EDTA, pH 7; the temperature was maintained at 6°.

This second valley which always appears in the plots from experiments run at the lower cell-loading and/or lower rotor speed conditions, we believe, is caused by a single higher *n*-mer in significant concentration. As expected, the presence of the higher *n*-mer species is reflected most strikingly in the $1/M_{z,app}$ function. The second minimum gives the ln *c vs.* r^2 plot of the data (Figure 8b) a nearly linear appearance with three barely discernible inflection points. This plot is further proof of the insensitivity of the conventional method of analysis, which would suggest that the solution in this experiment contained a monodisperse, ideal behaving solute.

Figure 9 displays $1/M_{w,app}$ distributions up to about 1.3 mg/ml from experiments made under a variety of conditions. They provide additional information about the properties of the higher *n*-mer species and its effect on the reciprocal apparent weight-average distribution throughout the liquid column. Curves a and b are from experiments under identical conditions except that in the run giving curve b, 350 μl of mineral oil was layered on top of the solution and dialysate thus increasing the hydrostatic pressure significantly throughout both liquid columns (from about 2 to 10 atm at the bottom of the columns). The expression of the second minimum is noticeably reduced in this experiment over that in the control run (curve a) suggesting that the higher *n*-mer, like the much larger synthetic myosin filament generated at low ionic strength (Josephs and Harrington, 1967) is labile to increased pressure.

Curves c and d illustrate the effect of run time on the amount of higher *n*-mer seen. In both experiments, speed and loading concentration were the same; however, the experiment producing curve d was allowed to continue an additional 3 days beyond the time required to reach sedimentation equilibrium. During this period, the relative amount of higher *n*-mer appears to have increased to the point of almost obscuring expression of the monomer–dimer valley.

Curve e summarizes results from one of a few experiments made with myosin in the absence of phosphate. Loss of definition in the higher *n*-mer valley is apparent suggesting the presence of more than one higher *n*-mer in significant concentration. The dimer upturn also occurs at higher weight average values indicating that there is more dimer present and that, therefore, k_2 is somewhat higher in the absence of PO_4^{2-}.

Curve f is derived from a run with myosin in the presence of phosphate at 10,000 rpm and a loading concentration of 0.79 mg/ml demonstrating the increased concentration of the *n*-mer under these intermediate run conditions. As rotor speed and loading concentration are further lowered, the higher *n*-mer valley increases in size and tends to nearly mask the expression of the monomer–dimer upturn (curve

g). Experiments carried out under these conditions were considered to be clearly inappropriate for the monomer–dimer analysis given earlier and were therefore excluded in the averaged results shown in Figure 4.

The variable expression of the higher *n*-mer, dependent on run time in addition to cell-loading concentration and rotor speed indicates that the heavier species is not in equilibrium with the M–D system. However, it may be the product of a reversible reaction but one so slow that chemical equilibrium is not achieved in the time required to reach nominal sedimentation equilibrium. Thus, the higher *n*-mer acts as though it were present at some fixed fraction of the total concentration, expressing itself more strongly within the low concentration range at sedimentation equilibrium at both lower speeds and lower cell-loading concentrations.

Very heavy species are also present causing the downward curvature of the reciprocal averages at radial positions close to the bottom of the column in experiments at low cell loading and low rotor speeds which have resolvable fringes in this region (as in curve g). The contribution of this material to the total protein mass is slight, however, since this fringe area represents no more than 1% or so of the total column length.

The double minima seen in the apparent reciprocal weight moments just described can be simulated by computer generated distributions for model systems. Figure 10 presents $1/M_{w,app}$ curves for a monomer–dimer reversible association obeying the three calculated parameter values in Table I with 20% by weight of an irreversible hexamer also present. The virial coefficients for all species are assumed to be the same. Because it is not in equilibrium with the M–D system, the influence of the higher *n*-mer on the molecular weight at any total concentration will depend on both cell-loading concentration and rotor speed. Solid curves are distributions for runs at 9000 rpm and various cell loadings. With decreasing cell-loading concentration, the influence of the higher *n*-mer is seen, first as a deflection, and then as a distinct second valley. At very low cell loadings, the second valley becomes dominant and obscures the monomer–dimer minimum. The dashed curve is the distribution from a hypothetical experiment with a cell-loading concentration equal to that which gave curve e, about 0.6 mg/ml, but run at 12,000 rpm. The monomer and dimer species are more effectively separated from the hexamer at the higher centrifugal field resulting in a much less perturbed $1/M_{w,app}$ distribution.

If the size of the higher *n*-mer is altered in these model systems, its expression in the $1/M_{w,app}$ *vs.* *c* function under the same run conditions is also altered. Figure 11 demonstrates the difference between the $1/M_{w,app}$ functions with tetramer and octamer present, again at 20% of the total concentration; curve e from the hexamer series (Figure 10) is also included. It can be seen that decreasing the size of the heavier species shifts the second minimum to lower concentrations, finally causing it to merge with the M–D upturn. Increasing *n*, however, causes the *n*-mer valley to become more distinct as it moves to higher concentrations and to increase the height of the intervening maximum.

The $1/M_{w,app}$ distributions from experiments at intermediate run conditions in most cases show a distinct second valley strongly suggesting that in the PO_4^{2-} solvent system, only one higher *n*-mer is present in significant concentration. Additional *n*-mers each exhibiting its valley at a different

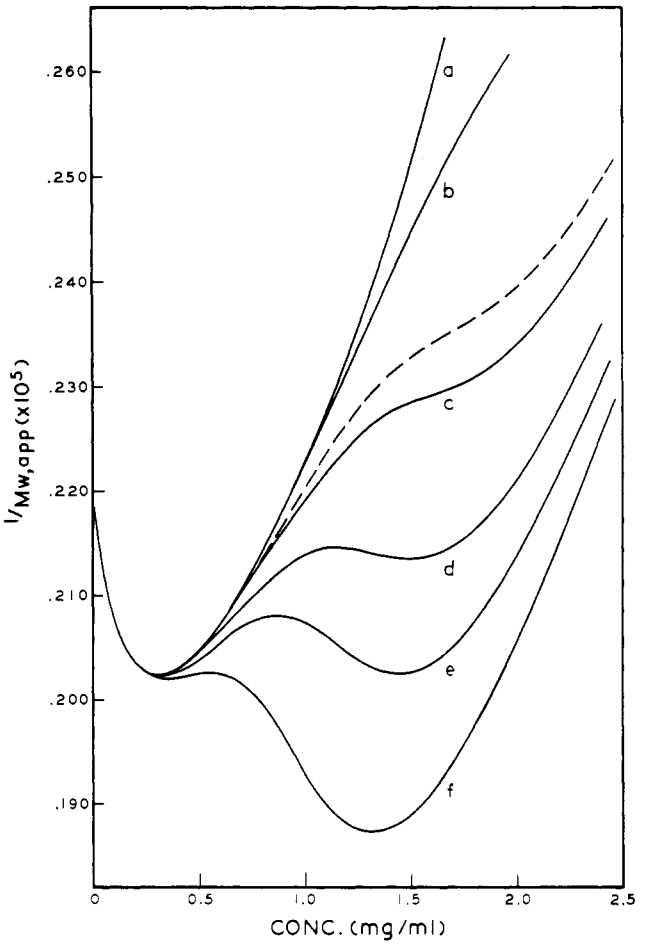

FIGURE 10: Simulated $1/M_{w,app}$ *vs.* concentration for M–D reversible association with 20% hexamer at different cell-loading concentrations. M_1, B, and K_2 values are from Table I; $B_{hexamer} = B_{M-D}$; 9000 rpm. Cell-loading concentrations were: (a) 10 mg/ml; (b) 1.56 mg/ml; (c) 0.91 mg/ml; (d) 0.67 mg/ml; (e) 0.56 mg/ml; (f) 0.43 mg/ml; (---) 0.54 mg/ml at 12,000 rpm.

concentration would tend to broaden and blur their net expression. A broad second valley is seen for example in the curve from the experiment made in KCl alone (Figure 9, curve e) suggesting that in this solvent more than one higher *n*-mer may be present.

If the virial coefficient for the heavier species were known or if it could be assumed to be the same as that found for the M–D system the size of the *n*-mer could be estimated from the $1/M_{app}$ *vs.* *c* functions. However, the virial coefficient for a higher *n*-mer made up of highly asymmetric particles is very probably quite different from the monomer value. On the basis of the results presented, it can only be said that in phosphate a higher *n*-mer is present at significant concentration which is very likely larger than tetramer and smaller than decamer.

Discussion

In light of the present findings some consideration of past efforts at determining the molecular weight of myosin is warranted. We believe that many of the conflicting values

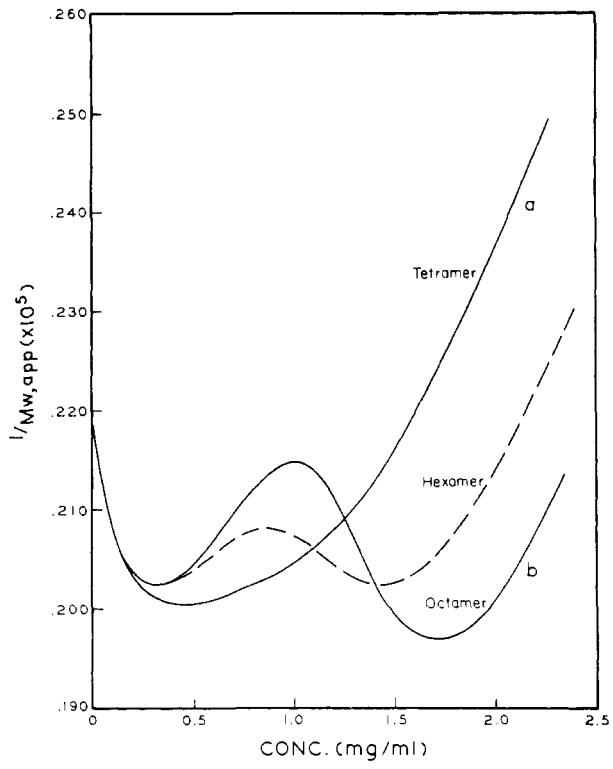

FIGURE 11: Simulated $1/M_{w,app}$ *vs.* concentration for a M–D reversible association with 20% of tetramer, hexamer, or octamer present. M_1, B, and K_2 equal values in Table I; $B_{n\text{-mer}} = B_{M-D}$; 9000 rpm: (a) 0.51 mg/ml with tetramer; (b) 0.64 mg/ml with octamer; (---) 0.56 mg/ml with hexamer (curve e, Figure 10).

reported in the literature have resulted from the peculiar properties of the reversible association pointing to reasonable but incorrect interpretations of data. Figure 7 illustrates why molecular weight data gathered within different concentration ranges can lead to radically different monomer weights. Consistent with the preliminary data, it is assumed for the purposes of this analysis that the characteristics of the M–D system in KCl alone closely approximate those found in the presence of PO_4^{2-}. A series of short-column, low-speed sedimentation equilibrium experiments (or Archibald approach-to-equilibrium runs) at various high cell-loading concentrations gives cell-average $1/M_{w,app}$ values tending to fall on a line (such as line a) which when extrapolated linearly to infinite dilution, would indicate a molecular weight of over 520,000 (Woods *et al.*, 1963; Kielley and Harrington, 1960; Mueller, 1964). Intermediate-speed (LaBar) runs would likewise give reciprocal weights on this line (*e.g.*, open square and circle in Figure 7 of Godfrey and Harrington, 1970). Results from experiments at both speed conditions, therefore, offer no hint of the presence of self-association, but do record the strong nonideality of the system.

Meniscus-depletion experiments with myosin analyzed by the ln c *vs.* r^2 plot method give values reflecting the middle data points of such plots, generally within the concentration range 0.3–0.6 mg/ml. Thus, the apparent molecular weights from such runs will be the values found in the upturn region of the monomer–dimer association (line b, Figure 7). Values in this range have been reported by Chung *et al.* (1967) who considered it unnecessary to extrapolate the apparent reciprocal weight at these very low concentrations to infinite dilution; their average value is 510,000. If the virial coefficient found by Woods *et al.* (1963) is assumed, this reciprocal value would fall on a line extrapolating to an infinite dilution weight of about 560,000. When the 21 high-speed experiments in phosphate are analyzed by the ln c *vs.* r^2 plot method, an average apparent weight-average molecular weight of 486,000 is obtained. This lower molecular weight reflects the lower amount of higher n-mer(s) present and perhaps also a somewhat smaller k_2 in the PO_4^{2-} solvent system. It falls on a line with values obtained by ln c *vs.* r^2 analysis of data from three intermediate-speed experiments in this solvent (solid triangle and circles, Figure 7 in Godfrey and Harrington, 1970).

It is interesting to note that Chung *et al.* (1967) reported that their ln c *vs.* r^2 plots were linear, despite the fact that the concentration range spanned was more than adequate to demonstrate downward curvature; the downward curvature is clearly apparent in plots covering a similar concentration range above the upturn (*e.g.*, Figure 6, Godfrey and Harrington, 1970). However, in the present study ln c *vs.* r^2 plots of data from the high-speed sedimentation equilibrium experiments also appear linear since they encompass the region of the minimum where there is relatively little change in $M_{w,app}$ with concentration. When the higher n-mer is expressed moderately—its valley comparable in size with that of the M–D upturn—the ln c *vs.* r^2 plot with its three inflection points is indistinguishable from a straight line.

Light-scattering results from myosin solutions at concentrations within the region of the minimum also lead to weights in the 470,000 to 520,000 range (Holtzer and Lowey, 1959). Full Zimm plots of scattering data from this concentration region, in common with ln c *vs.* r^2 plots, indicate a lack of concentration dependence for the molecular weight; early reports that myosin lacked a significant virial coefficient were based on this observation (Holtzer and Lowey, 1959; Blum and Morales, 1953). It was not until later sedimentation equilibrium studies were made at higher concentrations, away from the upturn, that the strong nonideal behavior of this molecule was discovered (Kielley and Harrington, 1960; Woods *et al.*, 1963; Mueller, 1964). Subsequent light-scattering experiments at higher concentrations confirmed this finding (Gellert and Englander, 1963; Tomimatsu, 1964).

The virial coefficient given in Table I is over twice the magnitude of any previously reported for myosin. This increased value for B could be due to significant binding of PO_4^{2-} ions and perhaps also to an increase in the net charge on the myosin molecule. More importantly, however, at the high rotor speeds employed in the meniscus-depletion experiments the higher n-mer is more effectively separated from the monomer and dimer species than at the lower speeds used in the Archibald and short-column techniques. Thus, the true magnitude of the nonideality inherent in the monomer–dimer system is revealed rather than being masked by the presence of the heavier species.

The myosin "dimer" (Holtzer, 1956; Holtzer and Lowey, 1959; Johnson and Rowe, 1960) reported to be present in aged myosin preparations and in fresh ones allowed to stand at room temperature for brief periods is clearly not the dimer species of this report. The former appears as a separate, faster moving peak in sedimentation velocity which sometimes

divides into two or more smaller peaks, identified as trimer or larger species. But, since these small *n*-mers form distinct boundaries, separate from the main boundary, they cannot be in reversible equilibrium with monomer. However, if these species were somewhat larger in size (hexamer, for instance), they could form separate distinguishable peaks and still be in reversible equilibrium with the M–D system (Nichol *et al.*, 1964; Cox, 1969). It is tempting to surmise that this faster sedimenting material is related not to the dimer, but to the higher *n*-mer species also found in the phosphate solvent. The slow formation of higher *n*-mer may also be responsible for the time dependent increase in the apparent weight-average molecular weight of myosin observed over extended periods (40–156 hr) (Gershman *et al.*, 1969). Definite conclusions on this point are, as yet, impossible. (See Methods for further comment on the problem of chemical equilibrium in sedimentation equilibrium experiments.)

The association constant (9.98 dl/g) for the myosin dimerization in the phosphate solvent is, as far as we are aware, the largest reported to date for a simple monomer–dimer system. At the concentrations normally employed for *in vitro* studies, most of the myosin by weight is in the dimer state (*e.g.*, in a 1% solution, over 70% of the myosin is dimerized). Albright and Williams (1968) have reported a k_2 of 8.10 dl/g for β-lactoglobulin at pH 2.58 and in 0.15 M NaCl–HCl. However, on a liter per mole basis, the two constants are quite different: 0.75×10^4 l./mole for the 18,000 molecular weight globular protein, but 22.9×10^4 l./mole for myosin; the molar free energies of association for the two systems reflect this difference also. Whether the association affinity under the high salt conditions bears any relationship to the affinity under physiological conditions is open to question. The association constant for the monomer–synthetic thick filament equilibrium is very sensitive to ionic strength (Josephs and Harrington, 1968). If this relationship holds to any degree for the monomer–dimer association, then k_2 under *in vivo* conditions could be very much higher than 9.98 dl/g.

An association constant cannot be reported for the higher *n*-mer since it is clear that this species had not reached chemical equilibrium with the M–D system. The possibility of the higher *n*-mer being an irreversible aggregate, albeit of specific size, cannot be ruled out, although the oil layering experiment (curves a and b, Figure 9) indicates a sensitivity to hydrostatic pressure which suggests reversibility. Still, pressure could be working only to retard the rate of aggregation rather than causing higher *n*-mer already formed to revert to the monomer and dimer state.

It is certainly possible, on theoretical grounds, for a monomer–higher *n*-mer equilibrium to be sensitive to pressure to the extent of unequivocal detection, even by the mild increase in hydrostatic pressure created by the overlayering of oil at the speeds employed in these studies. If the higher *n*-mer should possess the same per monomer increase in volume (~400 ml/mole) found for the filament, the association constant for a hexamer would be reduced by a factor of about 3 at 12,000 rpm with a full head of oil layered over the solution column (Josephs and Harrington, 1967, 1968). However, assuming the same $\Delta\bar{v}$ for the dimer would lead to a reduction in k_2 by a factor of only 1.4 under similar run conditions. In the oil layering experiment, the higher *n*-mer was reduced in concentration by a factor of about 2 and k_2 appeared to be unaffected; these results are consistent, therefore, with the above analysis. Work is in progress to further clarify the pressure dependency of this system.

What role the dimer and higher *n*-mer may have in the reactions leading to the formation of the filament cannot be defined at this time. In the synthetic filament equilibrium studies at low ionic strengths (Josephs and Harrington, 1966) no intermediates in significant concentration were detected. It is possible that the higher *n*-mer is stable only at high ionic strength; or it may be stable at low ionic strengths, as well, but does not build up in concentration under conditions which permit filament formation.

$$\mathrm{M} \rightleftharpoons \mathrm{D} \rightleftharpoons \text{higher } n\text{-mer} \rightleftharpoons \text{(blocked in high salt)} \rightleftharpoons \text{filament}$$

In the above scheme, the higher *n*-mer is not present in detectable concentrations as long as the reaction leading to filament can proceed at a reasonable rate. In high salt, however, filament will not form and the higher *n*-mer accumulates slowly as an end product of reaction.

The supposition that the dimer is composed of two myosin molecules associated in an antiparallel overlap configuration is attractive. Some years ago Rice (1963) published electron micrographs of dumbbell-shaped myosin aggregates which may well be related to the solvated dimer species of the present report. Antiparallel packing of myosin monomer units is thought to exist only in the smooth midsection of the thick filament (Huxley, 1963; Pepe, 1967). Elsewhere, in the cross-bridge region which constitutes the bulk of the filament mass, the evidence points to parallel packing of the monomer units. This fundamental distinction between the two modes of association may be reflected in the difference in sensitivity to ionic strength exhibited by the dimer and filament. If the dimer is, indeed, an antiparallel aggregate, the higher *n*-mer may be a trimer (or tetramer) of dimers gaining its stability in high salt by the juxtaposition of monomers from different dimer units in antiparallel association. As such, the higher *n*-mer could well be a substructure of the smooth central section which is thought to contain some 24 myosin molecules (Huxley, 1963; Pepe, 1967). Further studies will be required to clarify this question.

Finally, the implications of the very low monomer weight deserves comment. A weight of 458,000 g/mole would seem to rule out the three polypeptide chain model for the myosin molecule (Kielley and Harrington, 1960; Woods *et al.*, 1963). The molecular weight of myosin is required to fit the simple relationship: molecular weight $= n \times$ chain weight$/(1-y)$, where n is the number of large polypeptide chains, and y is the weight fraction of small polypeptide units bound noncovalently to myosin and constituting from 5 to 15% of the total mass (Dreizen *et al.*, 1967; Locker and Hagyard, 1967; Gershman *et al.*, 1969; Fredericksen and Holtzer, 1968; Gaetjens *et al.*, 1968; Gazith *et al.*, 1970). The origin, number, weight, and significance of the small chain material are still under study. Presently, this low molecular weight protein is defined only in terms of the conditions required to remove it from the bulk of the myosin, namely very high pH (above 10) or moderate levels of guanidinium chloride concentration. With the molecular weight, n, and y equal to 458,000 g/mole, 2, and 0.1, respectively, the chain weight is required to be 206,000 g/mole which is in good agreement with recent values for the major subunit of myosin (Woods *et al.*, 1963; Gershman *et al.*, 1969; Gazith *et al.*, 1970). Since the exact

amount of low molecular weight protein material is not known with certainty this figure could be somewhat higher or lower.

Acknowledgment

We are indebted to Dr. Robert Josephs for constructive criticism of this paper and for many useful suggestions.

References

Adams, E. T., Jr. (1965), *Biochemistry 4*, 1646.
Adams, E. T., Jr. (1967a), *Biochemistry 6*, 1864.
Adams, E. T., Jr. (1967b), Fractions, Palo Alto, Calif., Beckman Instruments, Inc., No. 3, p 1.
Adams, E. T., Jr., and Filmer, D. L. (1966), *Biochemistry 5*, 2971.
Adams, E. T., Jr., and Williams, J. W. (1964), *J. Amer. Chem. Soc. 86*, 3454.
Albright, D. A., and Williams, J. W. (1968), *Biochemistry 7*, 67.
Blum, J., and Morales, M. S. (1953), *Arch. Biochem. Biophys. 43*, 208.
Chung, C. S., Richards, E. G., and Olcott, H. S. (1967), *Biochemistry 6*, 3154.
Cox, D. J. (1969), *Arch. Biochem. Biophys. 129*, 106.
Dreizen, P., Gershman, L. C., Trotta, P. P., and Stracher, A. (1967), *J. Gen. Physiol. 50*, 85.
Frederiksen, D. W., and Holtzer, A. (1968), *Biochemistry 7*, 3935.
Gaetjens, E., Barany, K., Bailin, G., Oppenheimer, H., and Barany, M. (1968), *Arch. Biochem. Biophys. 123*, 82.
Gazith, J., Himmelfarb, S., and Harrington, W. F. (1970), *J. Biol. Chem.* (in press).
Gellert, M., and Englander, S. W. (1963), *Biochemistry 2*, 39.
Gershman, L. C., Stracher, A., and Dreizen, P. (1969), *J. Biol. Chem. 244*, 2726.
Godfrey, J. E., and Harrington, W. F. (1970), *Biochemistry 9*, 886.
Holtzer, A. (1956), *Arch. Biochem. Biophys. 64*, 507.
Holtzer, A., and Lowey, S. (1959), *J. Amer. Chem. Soc. 81*, 1378.
Huxley, H. E. (1963), *J. Mol. Biol. 7*, 281.
Johnson, P., and Rowe, A. J. (1960), *Biochem. J. 74*, 432.
Josephs, R., and Harrington, W. F. (1966), *Biochemistry 5*, 3473.
Josephs, R., and Harrington, W. F. (1967), *Proc. Natl. Acad. Sci. U. S. 58*, 1587.
Josephs, R., and Harrington, W. F. (1968), *Biochemistry 7*, 2834.
Kielley, W. W., and Harrington, W. F. (1960), *Biochim. Biophys. Acta 41*, 401.
Locker, R. H., and Hagyard, C. J. (1967), *Arch. Biochem. Biophys. 120*, 454.
Mueller, H. (1964), *J. Biol. Chem. 239*, 797.
Nichol, L. W., Bethune, J. L., Kegeles, G., and Hess, E. L. (1964), *Proteins 2*, 305.
Pepe, F. A. (1967), *J. Mol. Biol. 27*, 203.
Rice, R. V. (1963), *in* Biochemistry of Muscle Contraction, Gergely, J., Ed., Boston, Mass., Little, Brown, p 41.
Richards, E. F., Chung, C.-S., Menzel, D. B., and Olcott, H. S. (1967), *Biochemistry 6*, 528.
Roark, D. E., and Yphantis, D. A. (1969), *Proc. N. Y. Acad. Sci. 164*, 245.
Tomimatsu, Y. (1964), *Biopolymers 2*, 275.
Woods, E. F., Himmelfarb, S., and Harrington, W. F. (1963), *J. Biol. Chem. 238*, 2374.
Yphantis, D. A. (1964), *Biochemistry 3*, 297.